The Cryosphere Discuss., 6, 5069–5094, 2012
www.the-cryosphere-discuss.net/6/5069/2012/
doi:10.5194/tcd-6-5069-2012
© Author(s) 2012. CC Attribution 3.0 License.

The Cryosphere Discussions

This discussion paper is/has been under review for the journal The Cryosphere (TC).
Please refer to the corresponding final paper in TC if available.

Hindcasting to measure ice sheet model sensitivity to initial states

A. Aschwanden[1,2], **G. Aðalgeirsdóttir**[3], **and C. Khroulev**[1]

[1]Geophysical Institute, University of Alaska Fairbanks, Fairbanks, Alaska, USA
[2]Arctic Region Supercomputing Center, University of Alaska Fairbanks, Fairbanks, Alaska, USA
[3]Danish Meteorological Institute, Copenhagen, Denmark

Received: 12 November 2012 – Accepted: 13 November 2012 – Published: 6 December 2012

Correspondence to: A. Aschwanden (aaschwanden@alaska.edu)

Published by Copernicus Publications on behalf of the European Geosciences Union.

Abstract

Recent observations of the Greenland ice sheet indicate rapid mass loss at an accelerating rate with an increasing contribution to global mean sea level. Ice sheet models are used for projections of such future contributions of ice sheets to sea level, but the quality of projections is difficult to measure directly. Realistic initial states are crucial for accurate simulations. To test initial states we use hindcasting, i.e. forcing a model with known or closely-estimated inputs for past events to see how well the output matches observations. By simulating the recent past of Greenland, and comparing to observations of ice thickness, ice discharge, surface speeds, mass loss and surface elevation changes for validation, we find that the short term model response is strongly influenced by the initial state. We show that the dynamical state can be mis-represented despite a good agreement with some observations, stressing the importance of using multiple observations. Some initial states generate good agreement with measured mass time series in the hindcast period, and good agreement with present-day kinematic fields. We suggest hindcasting as a methodology for careful validation of initial states that can be done before making projections on decadal to century time-scales.

1 Introduction

Realistic projections of ice sheet response to a changing climate should be based on a physical understanding of the processes involved, rather than trend extrapolation of historical observations (Arthern and Hindmarsh, 2006). Ice sheet models integrate such physical process understanding. Similar to short-term weather forecasts, a realistic initial state is essential for accurate simulations of the future evolution of an ice sheet (Arthern and Gudmundsson, 2010). Previous studies have often used ice volume (Stone et al., 2010; Applegate et al., 2012; Rogozhina et al., 2011) for validation of the initial state. Spatially-rich observations, and their rates of change are, however, better metrics to evaluate the quality of initial states (Vaughan and Arthern, 2007).

TCD
6, 5069–5094, 2012

To test initial states we use hindcasting, i.e. forcing a model with known or closely-estimated inputs for past events to see how well the output matches observations. Here we evaluate three initial states for the Greenland ice sheet produced with the Parallel Ice Sheet Model (PISM) (Khroulev and the PISM Authors, 2012) by their response to climate forcing from the high-resolution regional climate model HIRHAM5 (Christensen et al., 2006) for the period 1989–2011. We validate these initial states using observations of ice thickness, ice discharge, surface elevation changes, surface speed observations, and time-series of mass changes.

The Fourth Assessment Report of the Intergovernmental Panel on Climate Change (IPCC) predicted Greenland ice sheet contribution of 1–12 cm to global mean sea-level rise due to climatic mass balance (sum of the surface and internal mass balances, Cogley et al., 2011) by 2100. Potential changes in ice discharge were not incorporated into these projections due to the limited ability of ice sheet models to simulate recent changes in the margin geometry and surface speeds (IPCC, 2007). Predicting the future of ice sheets remains a challenge (Vaughan and Arthern, 2007; Alley and Joughin, 2012). The ice sheet modeling community is addressing this challenge by improving on model physics (e.g. Bueler and Brown, 2009; Larour et al., 2012a; Seddik et al., 2012), implementing physically-based calving parametrizations (Levermann et al., 2012), and by applying inverse methods to recover difficult to observe ice sheet bed properties (e.g. Morlighem et al., 2010; Larour et al., 2012a), to name a few efforts. Thanks to advanced meshing techniques and high-resolution through parallelization, models can now better resolve margin geometry and narrow outlet glaciers, which is crucial to accurately model ice discharge (Durand et al., 2011).

However, available observations are insufficient to provide an initial state (Arthern and Gudmundsson, 2010). For example, while the ice viscosity is strongly temperature-dependent, the ice temperature field itself is poorly constrained by observations. As a consequence, initialization techniques must combine available observations of present and past conditions with physical models to produce a complete initial state of an ice sheet model.

TCD
6, 5069–5094, 2012

The paper is structured as follows: Sect. 2 describes data sets, initialization procedures, and hindcasting. Results are presented in Sect. 3 and discussed in Sect. 4. Conclusions are drawn in Sect. 5. The regional climate model HIRHAM5 and the ice sheet model PISM are described in the Supplement.

2 Methods

We obtain three initial states by using distinct approaches to modeling the 1989 state of the Greenland ice sheet, in each case based on forward modeling and assumptions about past climate. Below we describe how we obtain the three initial states.

We obtain the first initial state, "constant-climate", by running the model for 125 ka using mean values for 1989–2011 of 2-m air temperature and climatic mass balance from HIRHAM5. The 2-m air temperature serves as the boundary condition for the conservation of energy equation, and a lapse rate of 7.1 °C km^{-1} (Steffen and Box, 2001) is used to correct for differences between the fixed surface elevation that HIRHAM5 uses and the time evolving modeled elevation. No lapse rate correction is applied to the climatic mass balance. "Constant-climate" is in equilibrium with the present-day climate.

The second initial state, "paleo-climate", closely follows the SeaRISE initialization procedures (Bindschadler et al., 2012). To obtain this initial state we make the following modeling choices. First, we use a positive degree-day scheme to compute the climatic mass balance from surface temperature (Fausto et al., 2009) and precipitation (Ettema et al., 2009). The degree-day factors are the same as in Huybrechts (1998). Second, we account for paleo-climatic variations by applying a scalar anomaly term derived from the GRIP ice core oxygen isotope record (Dansgaard et al., 1993) to the temperature field (Huybrechts, 2002). Then we adjust mean annual precipitation in proportion to the mean annual air temperature change (Huybrechts, 2002). Finally, sea level forcing, which determines the land area available for glaciation, is derived from the SPECMAP marine δ^{18}O record (Imbrie et al., 1984).

TCD
6, 5069–5094, 2012

The third initial state, "flux-corrected", is similar to "paleo-climate", but the climatic mass balance has been modified during the last part of the simulation to obtain a present-day geometry in close agreement with observations (Supplement). This initial state is not in equilibrium with the applied forcing fields, and to prevent subsequent model drift a flux-correction is applied (Price et al., 2011). Such flux-correction methods have been applied in coupled ocean-atmosphere general circulation models (e.g. Sausen et al., 1988).

Our modeling goals are to produce physically-consistent initial states of the Greenland ice sheet in 1989 that mimic the overall dynamic state of the whole ice sheet. One cannot achieve agreement with all available observations except through introduction of many tunable parameters, which we do not do.

Also not all observed processes can be adequately represented in the model. For example increased ice discharge since the late 1990s has been observed (Joughin et al., 2004; Howat et al., 2007), and attributed to an increase in ocean temperatures (Holland et al., 2008; Murray et al., 2010). Unfortunately, theoretical models to predict such behavior are currently not available (Holland et al., 2008). Thus we reduce model complexity by excluding forcing at the ocean boundary.

Properties at the ice sheet bed cannot be directly observed. Ice sheet models may achieve a close fit to observed surface speeds by using data assimilation techniques that invert for a field of basal parameters, for example adjusting the value of the basal traction at each grid location (Morlighem et al., 2010; Price et al., 2011). The resulting parameter fields may not be applicable for prognostic simulations, however, as these parameters evolve with time. Moreover, validation cannot rely on the observations used in the data assimilation process (van der Veen, 1999).

In this work we adjust only three spatially-uniform scalar parameters (Supplement), controlling ice dynamics and basal processes, to achieve a good match with observed surface speeds. Thus observed surface speeds are not a part of the initialization procedure and can be used to validate the model.

TCD
6, 5069–5094, 2012

At the hindcast stage, all initial states are integrated forward in time from 1989 to 2011 using monthly fields of climatic mass balance and temperature computed by HIRHAM5, which is forced at its lateral boundaries with a reanalysis product for the period 1989–2011 (ERA-Interim). Note that identical dynamical parameter choices are used to produce all initial states, as well as in the 1989–2011 integration, allowing the influence of initialization procedures to be isolated. All hindcasts are carried out on a grid with horizontal resolution of 2 km.

The hindcasts are then compared to observations listed below.

- Ice thickness and ice volume (Griggs et al., 2012)
- Surface speeds derived from synthetic aperture radar (SAR) data from RADARSAT representing an average of the velocity maps for the period 2007–2010. The mean measurement and processing errors are less than $2\,\mathrm{m\,a^{-1}}$ in areas with low surface slope and additional slope-dependent error of 3 % in steeper areas (Joughin et al., 2010).
- Time-series of mass changes from the Gravity Recovery and Climate Experiment (GRACE) for the Greenland Ice Sheet, derived from the 10-day $1^\circ \times 1^\circ$ NASA GSFC mascon solutions for the period January 2004 to December 2010 (Luthcke et al., 2012). Using a linear least-squares fit a mass loss trend of $-223\,\mathrm{Gt\,a^{-1}}$ with an uncertainty of $\pm 14.3\,\mathrm{Gt\,a^{-1}}$ is obtained.
- Surface elevation changes measurements from NASA's Ice, Cloud and land Elevation Satellite (ICESat) for the period October 2003 until November 2009 (Sørensen et al., 2011; Sasgen et al., 2012).

TCD
6, 5069–5094, 2012

3 Results

3.1 1989 initial state

Figure 1 shows the simulated surface speeds of the three initialized states together with the SAR-derived speeds. All initial states show well-defined ice divides and fast flowing outlet glaciers, with largest differences between simulated and observed speeds occurring in outlet glaciers. The root mean square error (RMSE) is 43–46 $\mathrm{m\,a^{-1}}$ (Table 1), having a similar magnitude as obtained in a data assimilation study (38 $\mathrm{m\,a^{-1}}$, Price et al., 2011).

Compared to observed ice sheet volume ($2.93 \times 10^6\ \mathrm{km^3}$), numbers for two initialized states are larger, $3.18 \times 10^6\ \mathrm{km^3}$ (+9 %) and $3.38 \times 10^6\ \mathrm{km^3}$ (+16 %) for "constant-climate" and "paleo-climate", respectively (Table 1). For "flux-corrected", simulated ice volume is $2.96 \times 10^6\ \mathrm{km^3}$ (+1 %). However, observed ice thicknesses are used for initialization and are not available for validation.

Relative differences in ice thickness and surface speeds are shown in Figs. 2 and 3, respectively; absolute differences are shown in the Supplement.

Two initializations, constant-climate and paleo-climate, over-estimate ice thickness near the margin, but under-estimate ice thickness in the interior of the ice sheet and in North-West Greenland (Fig. 2). The flux-correction method used to obtain the "flux-corrected" initial state significantly reduces the mismatch between observed and simulated ice thickness except in coastal areas in South-East Greenland.

All three initializations under-estimate surface speeds in most major outlet glaciers (Fig. 3).

3.2 Hindcasts

The mass change time-series (Fig. 4) are normalized to the beginning of the GRACE period (January 2004). The GRACE time-series are compared to modeled ice mass changes using a correlation and linear regression analysis for the period January 2004

TCD
6, 5069–5094, 2012

to December 2011 (Table 1). The correlation coefficient, r, is greater than 0.92 in all experiments, indicating that both the amplitude and the phase of the mass change signal are well reproduced by the model. The detrended correlation coefficients, $\tilde{r}$, are 0.86 ("constant-climate", "paleo-climate") and 0.83 ("flux-corrected"); these are a measure of how well the seasonality is reproduced. Simulated mass loss trends are $-139\,\mathrm{Gt\,a^{-1}}$ for the hindcast based on the constant-climate initial state (subsequently shortened to constant-climate hindcast), $-299\,\mathrm{Gt\,a^{-1}}$ for the paleo-climate hindcast, and $-198\,\mathrm{Gt\,a^{-1}}$ for the flux-corrected hindcast, differing by a factor of more than 2. Mass loss trends are consistent with respect to the grid resolution (Supplement Table 1) for horizontal grid spacings $\leq 10\,\mathrm{km}$ (Supplement Fig. 2). Modeled mean ice discharge is -511, -581, and $-168\,\mathrm{Gt\,a^{-1}}$ for the constant-climate, paleo-climate and flux-corrected hindcast, respectively, over the period 1989–2011. None of the ice discharge time-series shows a significant trend. The modeled mass loss trend is thus due to the evolving climatic mass balance (Fig. 5).

Observed and simulated surface elevation changes between October 2003 and November 2009 are shown in Fig. 6. The constant-climate hindcast shows a thinning pattern similar to observations except for the drainage basins of Jakobshavn Isbræ, Helheim, and Kangerdlugssuaq. The paleo-climate and flux-corrected hindcasts show distinctively different patterns. Paleo-climate exhibits areas of both strong marginal thinning and thickening; near-marginal thickening occurs almost everywhere, except near the north-west coast. The hindcast based on the flux-corrected initialized state reveals strong marginal thickening and interior thinning.

4 Discussion

Despite having comparable ice volumes, the three initial states respond differently to the applied climate forcing, and the difference is significant, thus making ice volume a too weak validation metric.

TCD
6, 5069–5094, 2012

The simulations using a constant-climate and a paleo-climate initialization underestimate and over-estimate the mass loss trend, respectively, whereas the flux-corrected initialization shows a very good match with observations. Trend underestimation is expected because of the absence of ocean forcing that could lead to an increase in ice discharge. Consequently, we regard the paleo-climate initial state as unrealistic despite the seemingly good fit.

Compared to an observed cumulative mass change of −1695 Gt for the 2004–2010 period, simulated values are −1005 Gt ("constant-climate"), −2134 Gt ("paleo-climate"), and −1358 Gt ("flux-corrected"). van den Broeke et al. (2009) report an equal split between surface processes and ice dynamics for 2000–2008 mass loss. By assuming the same equal split between surface processes and ice dynamics during the 2004–2010 analysis period, we expect a simulated cumulative mass change of ~ -848 Gt from changes in climatic mass balance, corresponding to a trend of $\sim -113\,\mathrm{Gt\,a^{-1}}$. Of the three hindcasts only "constant-climate" has the right ballpark figure.

For the constant-climate and paleo-climate initialization, the simulated ice discharge compares well with an estimate of $-480\,\mathrm{Gt\,a^{-1}}$ (van den Broeke et al., 2009, Fig. S3) before ice discharge started to increase rapidly. However, the good agreement is a consequence of consistently over-estimating ice thickness (Fig. 2) and under-estimating surface speeds (Fig. 3). The flux-corrected initialization under-estimates the ice discharge as a result of under-estimating flow speeds in fast-flowing outlet glaciers. We find that simulated ice discharge is most sensitive to errors in ice thickness, which is in line with Larour et al. (2012b).

Surface elevation changes at Jakobshavn Isbræ, Helheim, and Kangerdlugssuaq are mostly attributed to changes in marine outlet dynamics (Howat et al., 2011) and are therefore not reproduced by our model. The constant-climate initialization is in equilibrium with its climate, and, consequently, surface elevation changes must result from the climate forcing, either directly through the applied climatic mass balance or, indirectly, through dynamical adjustment due to changes in climatic mass balance. For constant-climate and paleo-climate initializations, forcing is applied directly, whereas

TCD
6, 5069–5094, 2012

anomalies are used for the flux-corrected initialization. For the paleo-climate initialization this may result in a shock at the beginning of the hindcast. To study this effect we perform a fourth hindcast where the ERA-interim forcing is applied as anomalies relative to the climate forcing at the end of the paleo-climate initialization. Results reveal a mass loss trend of $-410\,\mathrm{Gt\,a^{-1}}$, greater than when the ERA-interim forcing is applied directly, with a surface elevation change pattern very similar to the flux-corrected hindcast (not shown).

Generally speaking, a model initialization may generate transients, both wanted (e.g. ongoing adjustments due to forcing history) and unwanted (e.g. from grid refinement), leading to a model drift. Even sufficiently long constant-climate initializations are not expected to be free of transients; for example, basal hydrology may prevent a steady-state configuration in the mathematical sense (e.g. Kamb et al., 1985). An approach to mitigate the effect of model drift involves calculating model drift and subtracting it from the experiment, implicitly assuming that legacy behavior does not feed back on the experiment (Bindschadler et al., 2012).

We calculate model drift by performing a reference run for each initial state where the mean climate of the last 10 yr of the initialization is applied. For the GRACE epoch, cumulative mass changes of −50 Gt ("constant-climate"), −281 Gt ("paleo-climate"), and −205 Gt ("flux-corrected") are attributed to model drift, corresponding to 5 %, 13 %, and 15 % of the total mass change, respectively. After subtracting model drift, simulated mass loss trends are $-132\,\mathrm{Gt\,a^{-1}}$ for the constant-climate hindcast, $-258\,\mathrm{Gt\,a^{-1}}$ for the paleo-climate hindcast, and $-169\,\mathrm{Gt\,a^{-1}}$ for the flux-corrected hindcast (Table 2).

The constant-climate hindcast exhibits the smallest drift, only minimally affecting the mass loss trend. In comparison, the drift of the paleo-climate and flux-corrected hindcasts are ∼ 5.5 × and 4 × higher. Now the mass loss of the flux-corrected is of the right order of magnitude, while "paleo-climate" is still too high. Ideally the flux-corrected hindcast should exhibit little to no drift at all, as flux-correction methods are supposed to compensate for drift. This is, however, not the case in our simulation. Similarly, Rahmstorf (1995) observes a residual drift in flux-corrected coupled ocean-atmosphere

TCD
6, 5069–5094, 2012

general circulation model (AOGCM) simulations. Improved physics, higher resolutions, and more physically-consistent coupling have rendered flux corrections mostly unnecessary in AOGCMs. Thus flux correction methods may be seen as a temporary remedy, until better coupling to the atmosphere is established.

Surface elevation changes corrected for model drift are shown in Fig. 7. The surface elevation changes pattern changes little when subtracting model drift, still exhibiting large transients not present in observations.

5 Conclusions

It has become clear that an initial state achieving a good fit with both spatially-rich surface speeds and rates of change of total ice mass may still misrepresent important characteristics (ice discharge and ice thickness are two examples). Additional metrics for validation are needed. Informally speaking, it is possible to "get the right result for the wrong reason".

Our analysis identifies spatially-rich time-series of observations as preferred validation metrics. Fortunately the number of both remotely-sensed and in situ observations is constantly growing. For example, spatially-distributed mass loss estimates from GRACE (e.g. Luthcke et al., 2012) and temporal variation in ice surface velocity (Joughin et al., 2010; Moon et al., 2012) are already available. Dated isochrones could be compared to the modeled age field. Future studies should take advantage of these data sets for validation.

In this study the dynamical state remains misrepresented by the "paleo-climate" and "flux-corrected" initial states, with potential implications for prognostic simulations. By using surface elevation changes as validation metric, it becomes evident that the "constant-climate" initialization performs significantly better than "paleo-climate" and "flux-corrected". Removing the model drift in this comparison changes the mass loss trend, but the spatial patterns are not significantly affected.

TCD
6, 5069–5094, 2012

We have demonstrated that ice sheet models are capable of transforming climate forcing into simulated mass loss from the ice sheet in a realistic way. Our model successfully reproduces the seasonal signal and decadal trends in mass loss as well as the velocity structure using only a few ice-sheet-wide parameters. The comparison of initialization strategies shows that the model response to climate forcing is sensitive to the initial state on decadal time scales, emphasizing the importance of well-validated initial states for reliable projections. We recommend thorough validation of initial states used for prognostic simulations, and hindcasting offers a viable validation strategy. Hindcasting is not limited to our particular choice of climate forcing and ice sheet model.

Further progress in ice-ocean coupling is necessary to also assess the variability in ice discharge, and future studies must quantify model sensitivities on longer, century to millennia, time-scales. The contribution of ice sheets may remain the major uncertainty in quantifying sea-level rise projections for the upcoming Fifth Assessment Report of IPCC (Vaughan and Arthern, 2007). The achievable accuracy of the model projections will depend on incompleteness in model physics, including calving mechanism, on uncertainties in boundary and initial states, and the quality of data available for validation (Vaughan and Arthern, 2007; Alley and Joughin, 2012). This work is a step towards more accurate initial states.

Supplementary material related to this article is available online at: http://www.the-cryosphere-discuss.net/6/5069/2012/tcd-6-5069-2012-supplement.pdf.

TCD
6, 5069–5094, 2012

Acknowledgements. Thanks to A. Arendt, T. Bartholomaus, E. Bueler, M. Fahnestock, R. Hock, D. Podrasky, and M. Truffer for stimulating discussions. S. B. Luthcke and I. Joughin provided GRACE and SAR data, respectively. J. A. Griggs provided basal topography and ice thickness. L. S. Sandberg Sørensen provided ICESat data, and R. Mottram and F. Forsberg provided HIRHAM5 forcing. M. Fahnestock provided the MODIS mosaic. This work was supported by NASA grant No. NNX09AJ38G, by a grant of HPC resources from the Arctic Region Supercomputing Center as part of the Department of Defense High Performance Computing Modernization Program, and by funding from the Ice2Sea programme from the European Union 7th Framework Programme, grant number 226375. Ice2sea contribution number ice2sea077.

References

Alley, R. B. and Joughin, I.: Modeling ice-sheet flow, Science, 336, 551–2, doi:10.1126/science.1220530, http://www.ncbi.nlm.nih.gov/pubmed/22556242, 2012. 5071, 5080

Applegate, P. J., Kirchner, N., Stone, E. J., Keller, K., and Greve, R.: An assessment of key model parametric uncertainties in projections of Greenland Ice Sheet behavior, The Cryosphere, 6, 589–606, doi:10.5194/tc-6-589-2012, 2012. 5070

Arthern, R. J. and Gudmundsson, G. H.: Initialization of ice-sheet forecasts viewed as an inverse Robin problem, J. Glaciol., 56, 527–533, 2010. 5070, 5071

Arthern, R. J. and Hindmarsh, R. C. A.: Determining the contribution of Antarctica to sea-level rise using data assimilation methods., Phil. Trans. R. Soc. A, 364, 1841–65, doi:10.1098/rsta.2006.1801, 2006. 5070

Bindschadler, R. A., Nowicki, S., Aschwanden, A., Choi, H., Fastook, J., Greve, R., Gutowski, G., Herzfeld, U., Jackson, C., Johnson, J., Khroulev, C., Levermann, A., Martin, M. A., Morlighem, M., Parizek, B. R., Pollard, D., Price, S. F., Ren, D., Saito, F., Sato, T., Seddik, H., Seroussi, H., Takahashi, K., Walker, R., and Wang, W.: Ice-Sheet Model Sensitivities to Environmental Forcing and Their Use in Projecting Future Sea-Level (The SeaRISE Project), J. Glaciol., in review, 2012. 5072, 5078

Bueler, E. and Brown, J.: The shallow shelf approximation as a "sliding law" in a thermomechanically coupled ice sheet model, J. Geophys. Res., 114, 1–21, doi:10.1029/2008JF001179, 2009. 5071

Christensen, O. B., Drews, M., Dethloff, K., Ketelsen, K., Hebestadt, I., and Rinke, A.: The HIRHAM Regional Climate Model. Version 5. Tech. Report 06-17, Tech. rep., DMI, Copenhagen, 2006. 5071

Cogley, J. C., Rasmussen, L. A., Arendt, A., Bauder, A., Braithwaite, R. J., Jansson, P., Kaser, G., Möller, M., Nicholson, M., and Zemp, M.: Glossary of Glacier Mass Balance and Related Terms, Tech. rep., UNESCO-IHP, Paris, 2011. 5071

Dansgaard, W., Johnsen, S. J., Clausen, H. B., Dahl-Jensen, D., Gundestrup, N. S., Hammer, C. U., Hvidberg, C. S., Steffensen, J. P., Sveinbjörnsdottir, A. E., Jouzel, J., and Bond, G.: Evidence for general instability of past climate from a 250-kyr ice-core record, Nature, 364, 218–220, 1993. 5072

Durand, G., Gagliardini, O., Favier, L., Zwinger, T., and le Meur, E.: Impact of bedrock description on modeling ice sheet dynamics, Geophys. Res. Lett., 38, 6–11, doi:10.1029/2011GL048892, http://www.agu.org/pubs/crossref/2011/2011GL048892.shtml, 2011. 5071

Ettema, J., van den Broeke, M. R., van Meijgaard, E., van de Berg, W. J., Bamber, J. L., Box, J. E., and Bales, R. C.: Higher surface mass balance of the Greenland ice sheet revealed by high-resolution climate modeling, Geophys. Res. Lett., 36, 1–5, doi:10.1029/2009GL038110, 2009. 5072

Fausto, R. S., Ahlstrøm, A. P., Van As, D., Bøggild, C. E., and Johnsen, S. J.: A new present-day temperature parameterization for Greenland, J. Glaciol., 55, 95–105, doi:10.3189/002214309788608985, 2009. 5072

Griggs, J. A., Bamber, J. L., , Hurkmans, R. T. W. L., Dowdesewell, J. A., Gogineni, S. P., Howat, I., Mouginot, J., Paden, J., Palmer, S., Rignot, E., and Steinhage, D.: A new bed elevation dataset for Greenland, The Cryosphere Discussions, 6, 4829–4860, doi:10.5194/tcd-6-4829-2012, http://www.the-cryosphere-discuss.net/6/4829/2012/, 2012. 5074

Holland, D. M., Thomas, R., de Young, B., Ribergaard, M. H., and Lyberth, B.: Acceleration of Jakobshavn Isbræ triggered by warm subsurface ocean waters, Nat. Geosci., 1, 659–664, doi:10.1038/ngeo316, 2008. 5073

Howat, I. M., Joughin, I., and Scambos, T. A.: Rapid changes in ice discharge from Greenland outlet glaciers., Science, 315, 1559–61, doi:10.1126/science.1138478, 2007. 5073

Howat, I. M., Ahn, Y., Joughin, I., van den Broeke, M. R., Lenaerts, J. T. M., and Smith, B.: Mass balance of Greenland's three largest outlet glaciers, 2000–2010, Geophys. Res. Lett., 38, 1–5, doi:10.1029/2011GL047565, 2011. 5077

TCD
6, 5069–5094, 2012

Huybrechts, P.: Report of the Third EISMINT Workshop on Model I intercomparison, Tech. rep., Grindelwald, Switzerland, 1998. 5072

Huybrechts, P.: Sea-level changes at the LGM from ice-dynamic reconstructions of the Greenland and Antarctic ice sheets during the glacial cycles, Quaternary Sci. Rev., 21, 203–231, doi:10.1016/S0277-3791(01)00082-8, 2002. 5072

Imbrie, J., Hays, J. D., Martinson, D. G., McIntyre, A., Mix, A. C., Morley, J. J., Pisias, N. G., Prell, W. L., and Shackleton, N. J.: The orbital theory of Pleistocene climate: Support from a revised chronology of the marine δ^{18}O record, in: Milankovitch and Climate: Understanding the Response to Astronomical Forcing, edited by: Berger, A., Imbrie, J., Hays, H., Kukla, G., and Saltzman, B., 269–305, D. Reidel Publishing, Dordrecht, 1984. 5072

IPCC: Climate Change 2007: The Physical Science Basis. Contribution of Working Group I to the Fourth Assessment Report of the Intergovernmental Panel on Climate Change, 2007. 5071

Joughin, I., Abdalati, W., and Fahnestock, M.: Large fluctuations in speed on Greenland's Jakobshavn Isbrae glacier., Nature, 432, 608–10, doi:10.1038/nature03130, 2004. 5073

Joughin, I., Smith, B., Howat, I. M., Scambos, T., and Moon, T.: Greenland flow variability from ice-sheet-wide velocity mapping, J. Glaciol., 56, 415–430, 2010. 5074, 5079, 5088

Kamb, B., Raymond, C. F., Harrison, W., Engelhardt, H., Echelmeyer, K. A., Humphrey, N. F., Brugman, M. M., and Pfeffer, W. T.: Glacier surge mechanism: 1982-1983 surge of Variegated glacier, Alaska, Science, 227, 469–79, doi:10.1126/science.227.4686.469, http://www.ncbi.nlm.nih.gov/pubmed/17733459, 1985. 5078

Khroulev, C. and the PISM Authors: PISM, a Parallel Ice Sheet Model: User's Manual, http://www.pism-docs.org, 2012. 5071

Larour, E., Seroussi, H., Morlighem, M., and Rignot, E.: Continental scale, high order, high spatial resolution, ice sheet modeling using the Ice Sheet System Model (ISSM), J. Geophys. Res., 117, 1–20, doi:10.1029/2011JF002140, 2012a. 5071

Larour, E. Y., Schiermeier, J., Rignot, E., Seroussi, H., Morlighem, M., and Paden, J.: Sensitivity Analysis of Pine Island Glacier ice flow using ISSM and DAKOTA., J. Geophys. Res., 117, doi:10.1029/2011JF002146, 2012b. 5077

Levermann, A., Albrecht, T., Winkelmann, R., Martin, M. A., Haseloff, M., and Joughin, I.: Kinematic first-order calving law implies potential for abrupt ice-shelf retreat, The Cryosphere, 6, 273–286, doi:10.5194/tc-6-273-2012, 2012. 5071

TCD
6, 5069–5094, 2012

Luthcke, S. B., Sabaka, T. J., Loomis, B. D., Arendt, A. A., McCarthy, J. J., and Camp, J.: Antarctica, Greenland and Gulf of Alaska land ice evolution from an iterated GRACE global mascon solution, J. Glaciol., submitted, 1–38, 2012. 5074, 5079, 5086, 5091

Moon, T., Joughin, I., Smith, B., and Howat, I. M.: 21st-Century Evolution of Greenland Outlet Glacier Velocities, Science, 693, 576–578, doi:10.1126/science.1219985, 2012. 5079

Morlighem, M., Rignot, E., Seroussi, H., Larour, E., Ben Dhia, H., and Aubry, D.: Spatial patterns of basal drag inferred using control methods from a full-Stokes and simpler models for Pine Island Glacier, West Antarctica, Geophys. Res. Lett., 37, 1–6, doi:10.1029/2010GL043853, 2010. 5071, 5073

Murray, T., Scharrer, K., James, T. D., Dye, S. R., Hanna, E., Booth, A. D., Selmes, N., Luckman, A., Hughes, a. L. C., Cook, S., and Huybrechts, P.: Ocean regulation hypothesis for glacier dynamics in southeast Greenland and implications for ice sheet mass changes, J. Geophys. Res., 115, 1–15, doi:10.1029/2009JF001522, http://www.agu.org/pubs/crossref/2010/2009JF001522.shtml, 2010. 5073

Price, S. F., Payne, A. J., Howat, I. M., and Smith, B. E.: Committed sea-level rise for the next century from Greenland ice sheet dynamics during the past decade, P. Natl. Acad. Sci. USA, 108, doi:10.1073/pnas.1017313108, 2011. 5073, 5075

Rahmstorf, S.: Climate drift in an ocean model coupled to a simple, perfectly matched atmosphere, Clim. Dyn., 11, 447–458, doi:10.1007/BF00207194, 1995. 5078

Rogozhina, I., Martinec, Z., Hagedoorn, J. M., Thomas, M., and Fleming, K.: On the long-term memory of the Greenland Ice Sheet, J. Geophys. Res., 116, 1–16, doi:10.1029/2010JF001787, 2011. 5070

Sasgen, I., van den Broeke, M., Bamber, J. L., Rignot, E., Sandberg Sørensen, L., Wouters, B., Martinec, Z., Velicogna, I., and Simonsen, S. B.: Timing and origin of recent regional ice-mass loss in Greenland, Earth Planet. Sc. Lett., 333-334, 293–303, doi:10.1016/j.epsl.2012.03.033, 2012. 5074

Sausen, R., Barthel, K., and Hasselmann, K.: Coupled ocean-atmosphere models with flux correction, Clim. Dyn., 2, 145–163, 1988. 5073

Seddik, H., Greve, R., Zwinger, T., Gillet-Chaulet, F., and Gagliardini, O.: Simulations of the Greenland ice sheet 100 years into the future with the full Stokes model Elmer/Ice, J. Glaciol., 58, 427–440, doi:10.3189/2012JoG11J177, http://www.igsoc.org/journal/58/209/t11J177.html, 2012. 5071

TCD
6, 5069–5094, 2012

Sørensen, L. S., Simonsen, S. B., Nielsen, K., Lucas-Picher, P., Spada, G., Adalgeirsdottir, G., Forsberg, R., and Hvidberg, C. S.: Mass balance of the Greenland ice sheet (2003-2008) from ICESat data — the impact of interpolation, sampling and firn density, The Cryosphere, 5, 173–186, doi:10.5194/tc-5-173-2011, 2011. 5074, 5093, 5094

Steffen, K. and Box, J. E.: Surface climatology of the Greenland ice sheet: Greenland Climate Network 1995-1999, J. Geophys. Res., 106, 33951–33964, 2001. 5072

Stone, E. J., Lunt, D. J., Rutt, I. C., and Hanna, E.: Investigating the sensitivity of numerical model simulations of the modern state of the Greenland ice-sheet and its future response to climate change, The Cryosphere, 4, 397–417, doi:10.5194/tc-4-397-2010, 2010. 5070

van den Broeke, M. R., Bamber, J. L., Ettema, J., Rignot, E., Schrama, E., van de Berg, W. J., van Meijgaard, E., Velicogna, I., and Wouters, B.: Partitioning recent Greenland mass loss, Science, 326, 984–986, doi:10.1126/science.1178176, 2009. 5077, 5092

van der Veen, C. J.: Evaluating the performance of cryospheric models, Polar Geography, 23, 83–96, 1999. 5073

Vaughan, D. G. and Arthern, R. J.: Why Is It Hard to Predict the Future of Ice Sheets?, Science, 315, 1503–1504, doi:10.1126/science.1141111, 2007. 5070, 5071, 5080

TCD
6, 5069–5094, 2012

Table 1. Initial states and model performance statistics. The root mean square error (RMSE) is given. Also listed are observed ice volume and GRACE trend (Luthcke et al., 2012), the correlation coefficient, r, and the detrended correlation coefficient, $\tilde{r}$. Ice volume is calculated by integrating ice thickness in space and multiplying by the density of ice (910 kg m^{-3}).

	observed	"constant-climate"	"paleo-climate"	"flux-corrected"
ice volume				
initial volume (10^6 km^3)	2.93	3.17	3.38	2.96*
ice thickness				
avg difference (m)		99	122	60*
rms difference (m)		199	244	19*
surface speed				
RMSE (m a^{-1})		43	46	45
mass trend				
trend (Gt a^{-1})	−223	−139	−299	−198
r (–)		0.92	0.99	0.99
$\tilde{r}$ (–)		0.86	0.86	0.83
RMSE (Gt)		130	104	62

* Ice thickness was used in the initialization, hence this metric is not available for validation, and only shown for comparison.

TCD
6, 5069–5094, 2012

Table 2. Simulated mass loss trends before and after drift removal for the three hindcasts.

	before drift correction (Gta^{-1})	after drift correction (Gta^{-1})	change (Gta^{-1})	(%)
"constant-climate"	−139	−132	+7	+5
"paleo-climate"	−299	−258	+40	+13
"flux-corrected"	−198	−169	+30	+15

TCD
6, 5069–5094, 2012

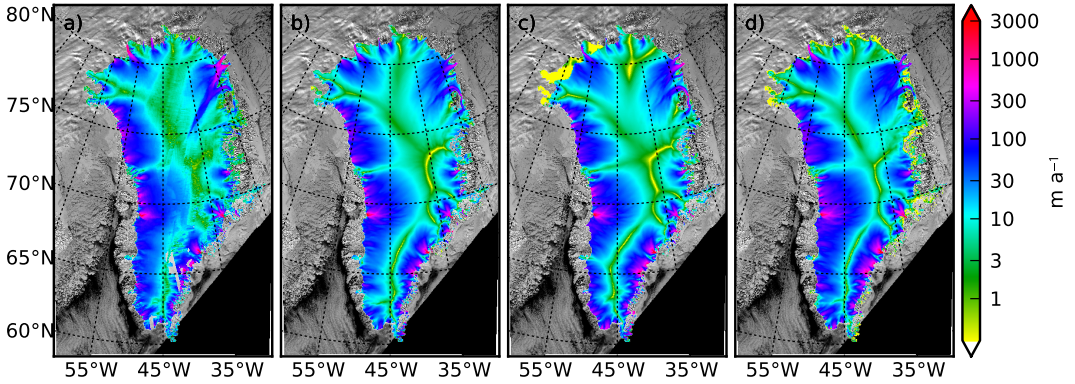

Fig. 1. Measured and modeled horizontal surface speeds. **(a)** SAR (Joughin et al., 2010). **(b)** Constant-climate hindcast. **(c)** Paleo-climate hindcast. **(d)** Flux-corrected paleo-climate hindcast. MODIS mosaic in the background is courtesy of M. Fahnestock. Values are in meters per year. Surface speeds are masked where observed ice thickness is less than 100 m.

TCD
6, 5069–5094, 2012

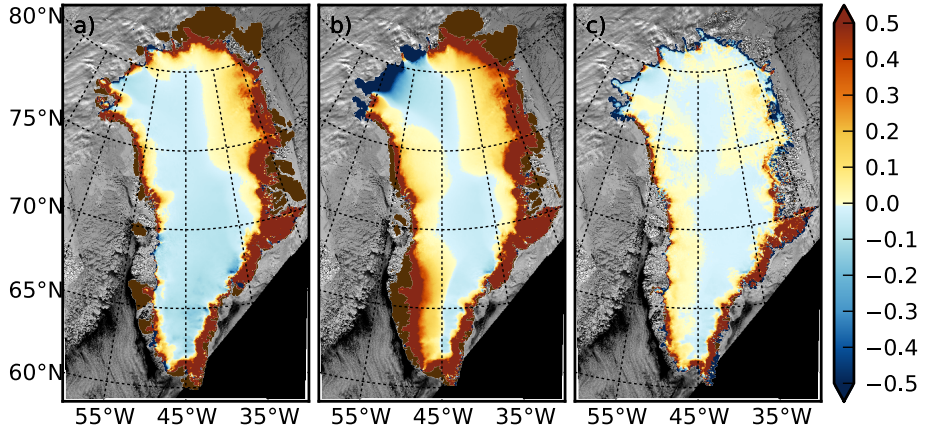

Fig. 2. Relative difference in ice thickness (model-observation)/observation. **(a)** Constant-climate hindcast. **(b)** Paleo-climate hindcast. **(c)** Flux-corrected paleo-climate hindcast (only shown for comparison, as ice thickness was part of the initialization). Blue and red colors indicate the model under- and over-estimates ice thickness, respectively. Brown color indicates areas where observed ice thickness is zero but the model simulates an ice thickness in excess of 100 m.

TCD
6, 5069–5094, 2012

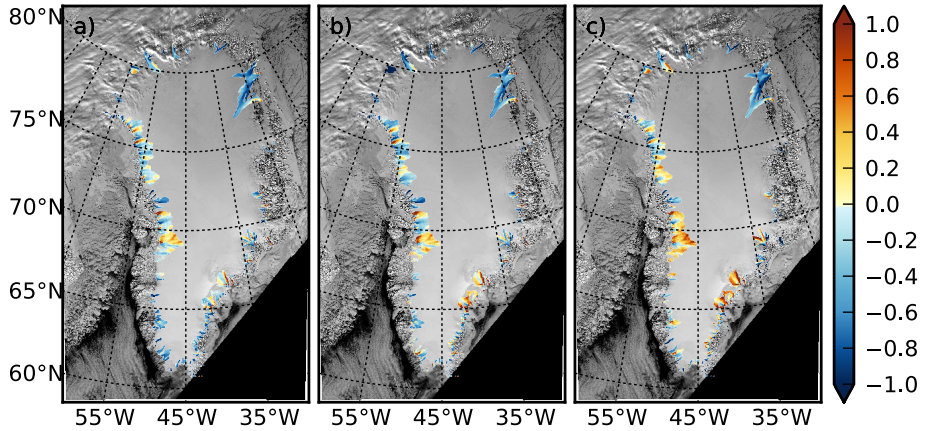

Fig. 3. Relative difference in surface speeds (model-observation)/observation. **(a)** Constant-climate hindcast. **(b)** Paleo-climate hindcast. **(c)** Flux-corrected hindcast. Blue and red colors indicate the model under- and over-estimates surface speed, respectively. Areas of observed surface speeds smaller than $100\,\mathrm{m\,a^{-1}}$ (92 % of observed speeds) are masked out because small absolute speed differences result in large relative speed differences. Also uncertainties in SAR-derived surface speeds are higher in slow-flowing areas.

TCD
6, 5069–5094, 2012

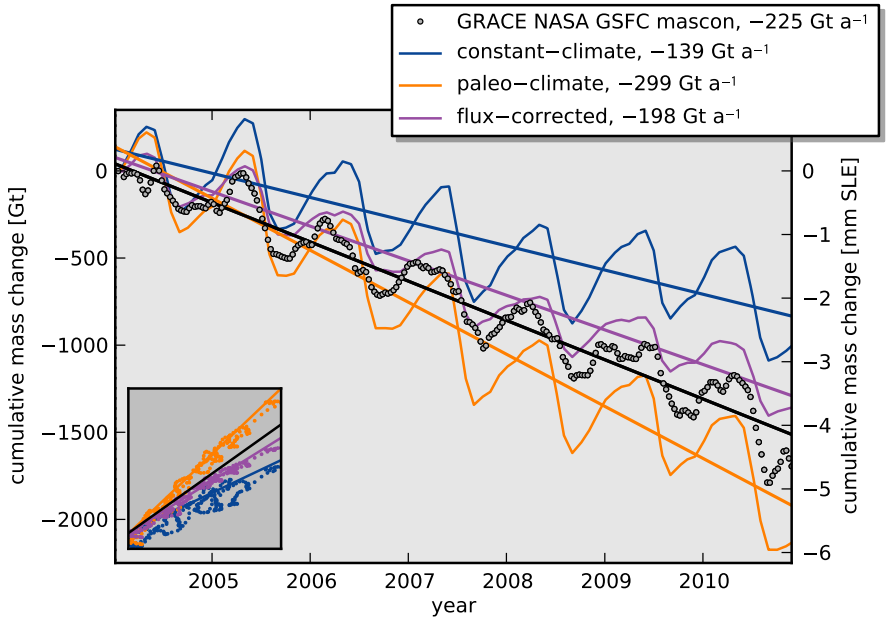

Fig. 4. Observed and modeled cumulative mass changes. 10-day solutions from GRACE observations (Luthcke et al., 2012) and simulated daily values starting from the three initial states. The inset figure shows the regression analysis; trends are given in the legend and correlation coefficients are listed in Table 1.

TCD
6, 5069–5094, 2012

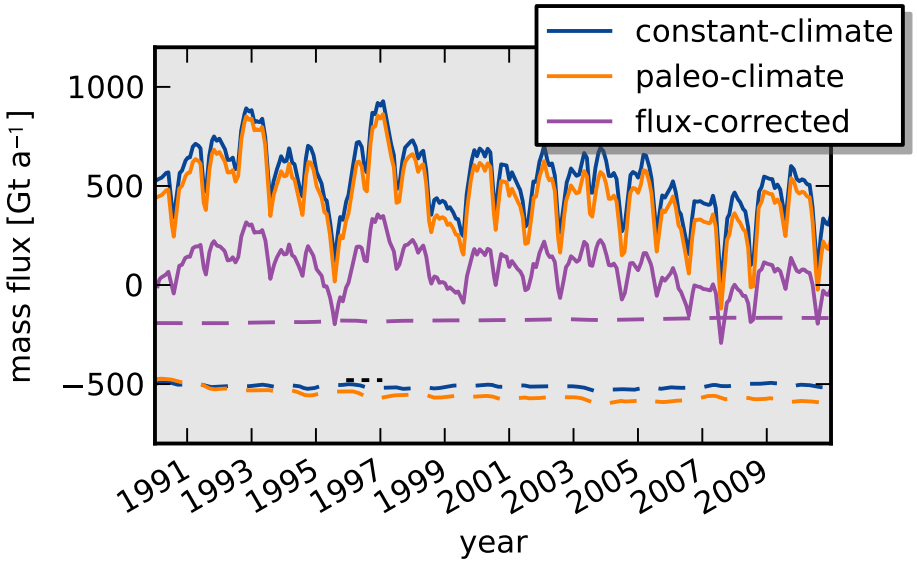

Fig. 5. Simulated mass fluxes from 1990 to 2010. Climatic mass balance (solid line) and ice discharge (dashed line). For comparison the ice discharge estimate for 1996 (van den Broeke et al., 2009) is shown (black dotted line). Time-series are smoothed with a 13-month running-average filter.

TCD
6, 5069–5094, 2012

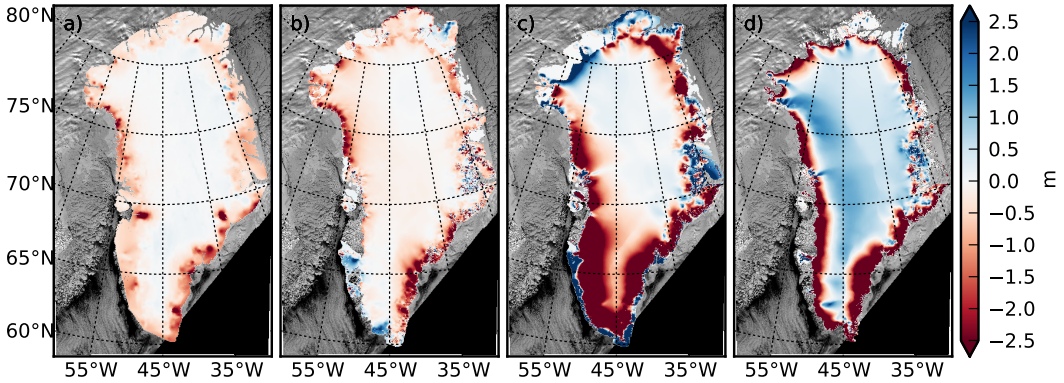

Fig. 6. Observed and modeled surface elevation change from October 2003 to November 2009. **(a)** ICESat (Sørensen et al., 2011). **(b)** Constant-climate hindcast. **(c)** Paleo-climate hindcast. **(d)** Flux-corrected paleo-climate hindcast. Values are in meters.

TCD
6, 5069–5094, 2012

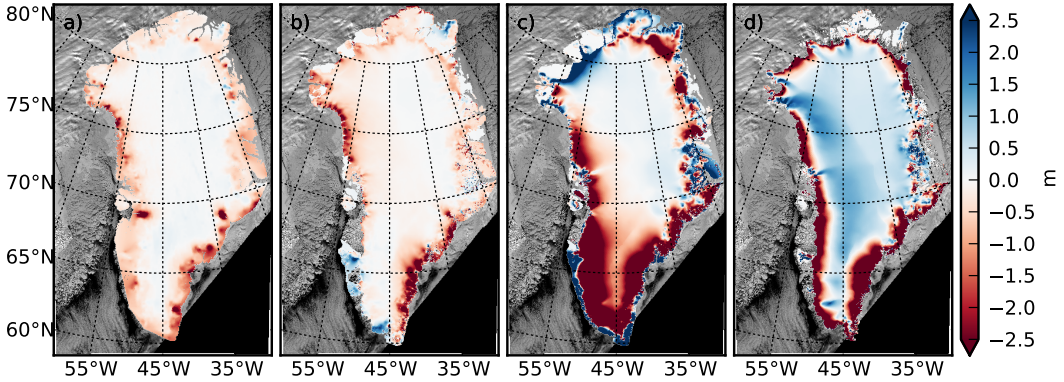

Fig. 7. Observed and modeled surface elevation change from October 2003 to November 2009 after subtracting the corresponding reference simulations. **(a)** ICESat (Sørensen et al., 2011). **(b)** Constant-climate hindcast. **(c)** Paleo-climate hindcast. **(d)** Flux-corrected hindcast. MODIS mosaic in the background is courtesy of M. Fahnestock. Values are in meters.

TCD
6, 5069–5094, 2012